

Compatible and Crystallization Properties of Poly(lactic acid)/Poly(butylene adipate-co-terephthalate) Blends

Jen-Taut Yeh,^{1,2,3} Chi-Hui Tsou,¹ Chi-Yuan Huang,⁴ Kan-Nan Chen,⁵ Chin-San Wu,⁶ Wan-Lan Chai⁷

¹Department and Graduate School of Polymer Engineering, National Taiwan University of Science and Technology, Taipei, Taiwan

²Faculty of Chemistry and Material Science, Hubei University, Wuhan, China

³Key Laboratory of Green Processing and Functional Textiles of New Textile Materials, Ministry of Education, Wuhan University of Science and Engineering, Wuhan, China

⁴Department of Materials Engineering, Tatung University, Taipei, Taiwan

⁵Department of Chemistry, Tamkang University, Tamsui, Taiwan

⁶Department of Biochemical Engineering, Kao Yuan University, Kaohsiung, Taiwan

⁷Department of Environmental Engineering, Vanung University, Tao-Yuan, Taiwan

Received 21 December 2008; accepted 9 June 2009

DOI 10.1002/app.30907

Published online 10 December 2009 in Wiley InterScience (www.interscience.wiley.com).

ABSTRACT: Differential scanning calorimetry (DSC), wide angle X-ray diffraction (WAXD) and dynamic mechanical analysis (DMA) properties of poly(lactic acid)/poly(butylene adipate-co-terephthalate) (PLA/PBAT) specimens suggest that only small amounts of poor PLA and/or PBAT crystals are present in their corresponding melt crystallized specimens. In fact, the percentage crystallinity, peak melting temperature and onset re-crystallization temperature values of PLA/PBAT specimens reduce gradually as their PBAT contents increase. However, the glass transition temperatures of PLA molecules found by DSC and DMA analysis reduce to the minimum value as the PBAT contents of PLA_xPBAT_y specimens reach 2.5 wt %. Further morphological and DMA analysis of PLA/PBAT specimens reveal that PBAT molecules are miscible with PLA

molecules at PBAT contents equal to or less than 2.5 wt %, since no distinguished phase-separated PBAT droplets and tan δ transitions were found on fracture surfaces and tan δ curves of PLA/PBAT specimens, respectively. In contrast to PLA, the PBAT specimen exhibits highly deformable properties. After blending proper amounts of PBAT in PLA, the inherent brittle deformation behavior of PLA was successfully improved. Possible reasons accounting for these interesting crystallization, compatible and tensile properties of PLA/PBAT specimens are proposed. © 2009 Wiley Periodicals, Inc. *J Appl Polym Sci* 116: 680–687, 2010

Key words: poly(lactic acid); poly(butylene adipate-co-terephthalate); compatibility; crystallization; blend

INTRODUCTION

Poly(lactic acid) (PLA) resins are well known as the biodegradable, linear aliphatic thermoplastics, which can be produced from renewable resources. However, their brittleness, slow crystallization, and hydrolysis properties limit their usage in many applications. In fact, they are difficult for film-blowing or extrusion unless carefully controlling their moisture contents and processing conditions. On the other hand, PLA resins were often blended with aliphatic amide¹ and other inorganics² such as talc, sodium stearate and calcium lactate to improve their crystallization rates and processability. Joo et al.¹ found that the overall crystallization rates of PLA

resins increased significantly with the addition of *N,N*-ethylenebis (1,2-hydroxystearamide), because the additives can serve as a nucleating agent during the very early crystallization stage of the PLA resins. Similar nucleating effects were also reported for those inorganic added PLA resins during their crystallization processes.²

Other than the organic and inorganic additives, several investigators^{3–7} found that poly(ethylene glycol) (PEG) resin can also serve as an effective polymeric plasticizer to facilitate the crystallization rates of the PLA resins. Lai et al.⁵ reported that PEG accelerated the crystallization ability of PLA, while the cold crystallization temperatures of PLA molecules decreased significantly after the addition of PEG. Further investigation found that, after addition of PEG, the spherulite growth rates and nucleation densities of PLA molecules increased and decreased, respectively, during the isothermal crystallization at 120°C of PLA/PEG blends.^{5–7} Another feasible approach to improve the flexible and toughness properties of PLA is to incorporate a biocompatible

Correspondence to: W.-L. Chai (chai@mail.vnu.edu.tw).

Contract grant sponsor: Department of Industrial Technology, Ministry of Economic Affairs; contract grant number: 95-EC-17-A-11-S1-057.

flexible polymer into the relatively brittle PLA matrix. As reported in the literatures,^{8–27} many biodegradable flexible resins, such as poly(ethylene oxide) (PEO),^{8–12} poly(ϵ -caprolactone) (PCL),^{13–18} poly(vinyl acetate) (PVAc),¹⁹ poly(hydroxyl butyrate) (PHB),^{20–24} poly(butylenes succinate) (PBS)^{25–27} were melt-blended with PLA to improve the flexibility (e.g., elongation at break (ϵ_f)) of the PLA blend. For instance, ϵ_f values of PLA/PEO blends increase from 5% to more than 500%, as their PEO contents increase from 0 to 20 wt %. Similarly, the ϵ_f values of PLA/PVAc blends reach 225% after blending only 5 wt % of PVAc in PLA. In contrast, no significant improvement in ϵ_f values and flexibility was found, when PLA was blended with varying amounts of PCL, PHB and PBS resins, respectively. The ϵ_f values of PLA/PHB blends reach merely about 28% even after adding 60 wt % of PHB in PLA. The ϵ_f values of PLA/PCL blends are always less than 10% when the PCL contents are equal to or less than 30 wt %. In fact, a phase-separated morphology was identified for all PLA/PCL blends prepared in their study.¹⁸ Presumably, the poor flexibility of these PLA blends is attributed to the poor compatibility and phase separation of PLA phases with those of PCL, PHB, and PBS resins, respectively.^{15–18,24–27}

Poly(tetramethylene adipate-co-terephthalate) (PTAT)²⁸ and Poly(butylene adipate-co-terephthalate) (PBAT)^{29–31} are biodegradable aliphatic/aromatic copolyesters, which exhibit higher hydrophilicity and better processability than other biodegradable polyesters. They also offer superior adhesion and are compatible with many other natural polymers,²⁸ wherein the presence of carbonyl groups in PTAT and PBAT makes them miscible or partial-miscible with PLA and/or other natural polymers after melt-blending. However, as evidenced by dynamic mechanical analysis,³² PTAT is not compatible with PLA molecules when PTAT contents are equal to or more than 50 wt %, in which the glass transition temperature peaks of PTAT and PLA present in the PLA/PTAT solution-casted film are away from each other than those observed between pure PLA and PBAT specimens. In contrast, PTAT is only partially compatible with PLA molecules even when PTAT contents reach about 25 wt %, at which the glass transition temperature peaks of PBAT and PLA present in the PLA/PTAT solution-casted film are slightly closer to each other than those observed between pure PLA and PTAT specimens. The σ_f values of PLA/PTAT specimens reduce significantly from 28.1 to 24.6 MPa although the ϵ_f values increase from 19.3 to 97.0%, as their PTAT contents increase from 0 to 25 wt %.

The repeating units of PBAT molecules are longer and more flexible than those of the PTAT molecules,

wherein PBAT molecules are synthesized from a longer monoester monomer. Presumably, the molecular structures of PBAT resins are more miscible with PLA than those of the PTAT molecules during the melt-blending processes. In fact, the processability of PBAT was reported to be comparable to low density of polyethylene (LDPE) with less ecological problem when disposed.³² Jiang et al.³¹ reported that, the impact strength of PLA/PBAT specimens increase dramatically from 2.6 to 4.4 GPa although their tensile strengths reduce from 63 to 47 MPa, after adding 20 wt % of PBAT in PLA. Further thermal and morphological studies suggest that PLA and PBAT molecules are not miscible but phase-separated in PLA/PBAT blends with PBAT contents varying from 5 to 20 wt %. However, possible reasons accounting for the immiscible and/or partial miscible behavior of PLA/PBAT or PLA/PTAT blends were not revealed. In this investigation, varying compositions of PLA/PBAT resins were prepared by melt-blending. The compatible, crystallization and tensile properties of PLA/PBAT blends with varying compositions were investigated. Possible reasons accounting for the interesting compatible, crystallization and tensile properties of the PLA/PBAT blends observed in this study were reported.

EXPERIMENTAL

Materials and sample preparation

The PLA and PBAT resins used in this study were obtained from Cargill Dow and BASF Corporation, respectively. The PLA/PBAT blend specimens were prepared by melt-blending PLA and PBAT resins using a SU-70 Plasti-Corder Mixer, which was purchased from Suyuan science and Technology Corporation, Chang Zhou, China. Before melt-blending, the PLA and PBAT resins were dried in a vacuum oven at 80°C for 3 h and 30°C for 12 h, respectively. The dried components of PLA/PBAT at varying weight ratios were then melt-blended in the Plasti-Corder Mixer. During each melt-blending process, the Plasti-Corder Mixer was operated at 190°C and a screw speed of 250 rpm for 3 min. The compositions of the melt-blended PLA/PBAT specimens prepared in this study were summarized in Table I. The hot-pressed film specimens used for tensile tests, dynamic mechanical, thermal, morphology and Wide angle X-ray diffraction analysis were prepared by hot-pressing the vacuum dried PLA and PLA/PBAT resins prepared above at 190°C and 10 MPa for 2 min and then cooled in a refrigerator at –18°C at a cooling rate of 20°C/s for 10 min.

TABLE I
The Compositions of the PLA_xPBAT_y Specimens

Sample code	PLA contents (wt %)	PBAT contents (wt %)
PLA	100	0
PLA _{97.5} PBAT _{2.5}	97.5	2.5
PLA ₉₅ PBAT ₅	95.0	5.0
PLA _{92.5} PBAT _{7.5}	92.5	7.5
PLA ₉₀ PBAT ₁₀	90	10
PLA ₈₅ PBAT ₁₅	85	15
PLA ₈₀ PBAT ₂₀	80	20
PBAT	0	100

Dynamic mechanical analysis

The hot-pressed specimens with 0.2 mm thickness were then sectioned into a rectangular strip with a dimension of 9 mm × 22 mm. The rectangular strips were then used as the specimens for all dynamic mechanical analysis (DMA) tests. The DMA experiments were operated at a frequency of 1 Hz, a heating rate of 3°C/min and under flowing N₂ atmosphere. The experiments were performed using a tensile mode and in a temperature range from -120 to 170°C.

Thermal properties

The isothermal crystallization behavior of PLA/PBAT specimens was performed using a Perkin-Elmer Pyris 1 differential scanning calorimetry (DSC) instrument under flowing nitrogen at a flow rate of 50 mL/min. The instrument was calibrated using the pure indium. Samples weighing about 15 and 0.5 mg were hermetically sealed in standard aluminum sample pans for glass transition and melting temperature determination of each specimen, respectively. Samples were first heated from -50°C to 200°C at a heating rate of 40°C/min and kept at 200°C for 10 min in order to remove any nuclei that might act as seed crystals. The fully melted samples were then cooled to -50°C at a cooling rate of 100°C/min and then scanned from -50°C to 200°C at a heating rate of 40°C/min.

The percentage crystallinity (X_c) values of PLA in PLA/PBAT specimens were estimated using baselines drawn from 95 to 190°C and a perfect heat of fusion (ΔH_m^0) of PLA of 93 J/g.³³ In which, the X_c values of PLA in PLA/PBAT specimens are evaluated as follows:

$$X_c (\%) = \frac{\Delta H_c}{(1 - \phi)\Delta H_m^0} \times 100$$

where ΔH_c is the net melting enthalpy of crystallization of PLA/PBAT specimens obtained by subtracting the enthalpy values of those of the re-

crystallization exotherms and ϕ is the weight fraction of PBAT in PLA/PBAT specimens.

Tensile properties

The tensile properties of the hot-pressed PLA and PLA/PBAT specimens were determined using a Shimadzu tensile testing machine model AG-10KNA at 25°C and a crosshead speed of 50 mm/min. A 35 mm gauge length was used during each tensile experiment. The dimensions of the dog-bone shaped specimens were prepared according to ASTM D638 type IV standard. The values of tensile strength and elongation at break were obtained based on the average tensile results of at least five tensile specimens.

Morphology analysis

The morphology of the hot-pressed PLA and PLA/PBAT specimens were observed using a Hitachi S-3000N scanning electron microscope (SEM). The fracture surfaces of the tested tensile specimens were gold-coated at 15 keV for 10 s before SEM examinations.

Wide angle X-ray diffraction properties

The wide angle X-ray diffraction (WAXD) properties of the hot-pressed PLA and PLA/PBAT specimens were determined using a Rigaku Analytical X-ray (D/MAX-III) diffractometer equipped with a Ni-filtered CuK α radiation operated at 3 kV. The specimen with 1 mm thickness was maintained stationary at 25°C and scanned in the reflection mode from 2 to 50° at a scanning rate of 5° min⁻¹.

RESULTS AND DISCUSSION

DSC analysis

Typical DSC thermograms of PLA, PBAT and PLA_xPBAT_y specimens scanned at 40°C/min were summarized in Figure 1. As shown in Figure 1(a), a thermal transition at temperatures near 60°C was observed in the DSC thermograms of PLA specimen, which is generally recognized as the glass transition temperature (T_g) of PLA resins.^{34,35} In addition to the glass temperature transition, a melting endotherm with a peak temperature at 169.8°C was found on the thermogram of PLA specimen. In contrast, one can barely find the melting endotherm on the thermogram of PBAT specimen in Figure 1(h), wherein a broad but nearly vanished melting endotherm with a peak temperature at around 108°C was found. After blending PBAT in PLA resins, the percentage crystallinity (X_c) and melting temperature (T_m) values of PLA_xPBAT_y specimens reduce

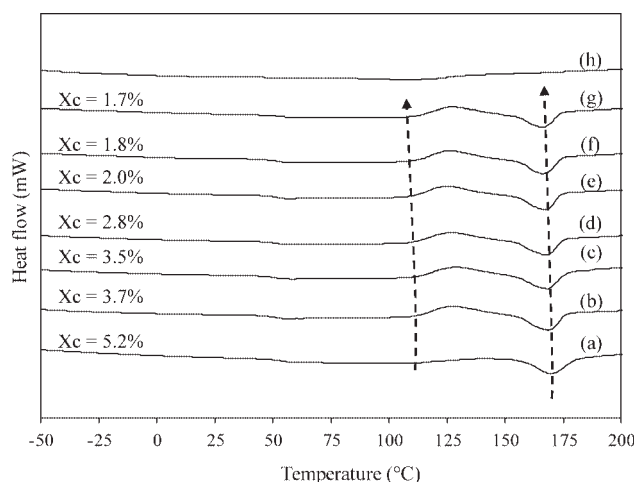


Figure 1 DSC thermograms of (a) PLA, (b) PLA_{97.5}PBAT_{2.5}, (c) PLA₉₅PBAT₅, (d) PLA_{92.5}PBAT_{7.5}, (e) PLA₉₀PBAT₁₀, (f) PLA₈₅PBAT₁₅, (g) PLA₈₀PBAT₂₀ and (h) PBAT specimens scanned at 40°C/min.

gradually as their PBAT contents increase (see Fig. 1 and Table II). Moreover, the T_g values of PLA molecules reduce from 62.3 to 58.6°C as the PBAT contents present in PLA_xPBAT_y specimens increase from 0 to 2.5 wt %. However, the T_g values of PLA molecules increase reversely from 58.6 to 60.8 and 61.2°C as the PBAT contents of PLA_xPBAT_y specimens increase from 2.5 to 5 and 20 wt %. On the other hand, it is worth noting that distinguished exotherms with onset temperatures (T_{onset}) near 114.5°C and 105–109°C were found on the DSC thermograms of the PLA and PLA_xPBAT_y specimens, respectively [Fig. 1(a–g)]. In fact, the onset temperatures of the exotherms of PLA_xPBAT_y specimens reduce from 109.1 to 105.0°C, as their PBAT contents increase from 2.5 to 20 wt %. The exotherms observed for PLA and PLA_xPBAT_y specimens are most likely due to the re-crystallization of PLA molecules during the second heat-scanning processes. However, the PBAT molecules are present mostly as melt state, as the temperatures are near the T_{onset} of PLA (c.a. 114.5°C) during their cooling processes. Instead of facilitating nucleation of PLA, the phase-separated PBAT molecules inhibit nucleation crystallization or re-crystallization of PLA, because they are present as melt state at temperatures near the T_{onset} of PLA. Moreover, less perfect PLA crystals with lower T_m are expected to grow as the crystallization or re-crystallization temperatures are lower. As a consequence, the values of X_c , T_m , and T_{onset} of PLA_xPBAT_y specimens reduce significantly as their PBAT contents increase.

Morphology analysis

Typical SEM micrographs of the fracture surfaces of PLA and PLA_xPBAT_y tensile specimens are shown

in Figure 2. As shown in Figure 2(a), relatively brittle and smooth fracture surface morphology was found on the fracture surface of the PLA specimen. In contrast, much coarser with significant plastic deformed debris was found on the fracture surface of PBAT specimen [Fig. 2(h)]. After blending PBAT in PLA resins, many demarcated phase-separated PBAT droplets were found dispersing on the fracture surfaces of the PLA_xPBAT_y specimens, as their PBAT contents are equal to or more than 5 wt % [Fig. 2(c–g)]. In fact, the sizes of the phase-separated PBAT droplets increase significantly with increasing the PBAT contents. However, a relatively smooth morphology without visibly phase-separated PBAT phases was found on the fracture surface of the PLA_{97.5}PBAT_{2.5} specimen. These interesting morphological results clearly suggest that PBAT molecules are not miscible and phase-separated with the PLA molecules after blending equal to or more than 5 wt % of PBAT in PLA resin. However, at PBAT contents equal to or less than 2.5 wt %, the PBAT molecules appear to be miscible with PLA molecules without clearly phase-separated PBAT phases.

Dynamic mechanical analysis (DMA)

Figure 3 exhibits the temperature dependence of the $\tan \delta$ curves of PLA, PBAT and PLA_xPBAT_y specimens. Two distinct transition peaks at temperatures near 74°C and –26°C were found on the $\tan \delta$ curves of PLA and PBAT specimens, respectively [Fig. 3(a,h)]. Similar to those found in the literatures,^{33,34} the transition peak near 74°C is recognized as the dynamic glass transition temperature (dynamic T_g) of PLA. The transition peak near –26°C is most likely originated from the glass transition motions of PBAT molecules. After blending PBAT in PLA resins, the PLA glass transitions were always observed on the $\tan \delta$ curves of PLA_xPBAT_y

TABLE II
Glass Transition (T_g), Melting (T_m) Temperatures and Onset (T_{onset}) Temperatures of the Re-crystallization Exotherms of PLA, PBAT, and PLA_xPBAT_y Specimens Evaluated from DSC and DMA Measurements

Sample code	DSC		DMA	
	T_g (°C)	T_{onset} (°C)	T_m (°C)	^a T_g (°C)
PLA	62.3	114.5	169.8	73.8
PLA _{97.5} PBAT _{2.5}	58.6	109.1	168.5	69.5
PLA ₉₅ PBAT ₅	60.8	109.0	168.2	71.9
PLA _{92.5} PBAT _{7.5}	60.9	107.0	167.8	72.3
PLA ₉₀ PBAT ₁₀	61.0	106.3	167.1	72.6
PLA ₈₅ PBAT ₁₅	61.2	105.7	166.3	72.7
PLA ₈₀ PBAT ₂₀	61.2	105.0	165.5	72.7
PBAT	–15.9	–	108.0	–26.1

^a The dynamic glass transition temperature (dynamic T_g).

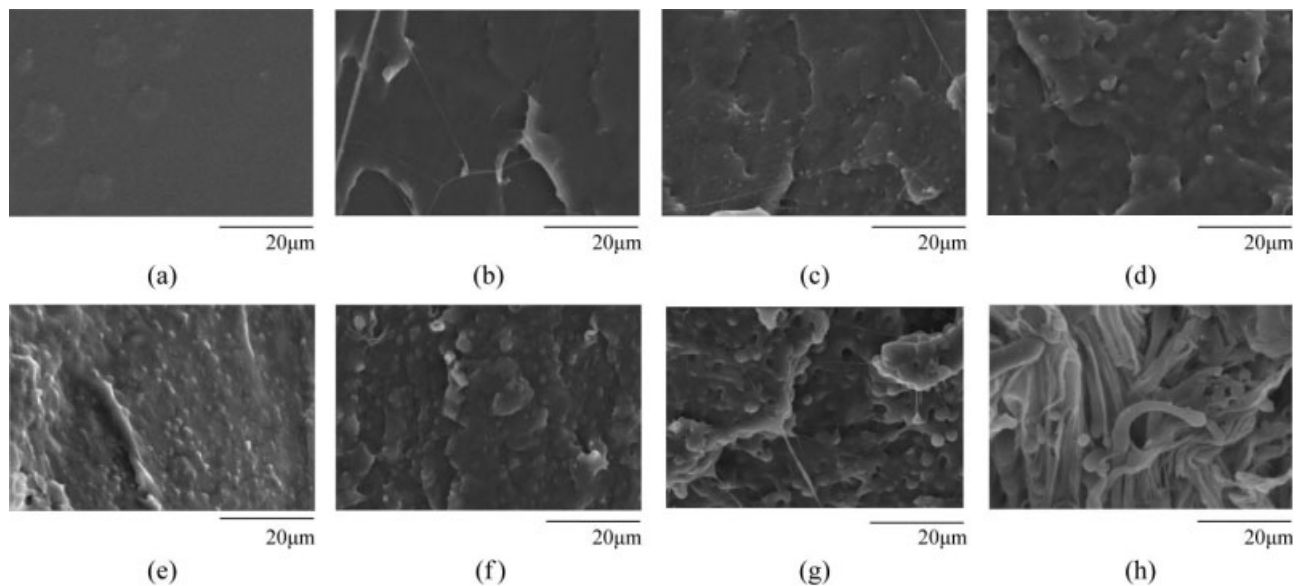


Figure 2 SEM micrographs of the fracture surfaces of (a) PLA, (b) PLA_{97.5}PBAT_{2.5}, (c) PLA₉₅PBAT₅, (d) PLA_{92.5}PBAT_{7.5}, (e) PLA₉₀PBAT₁₀, (f) PLA₈₅PBAT₁₅, (g) PLA₈₀PBAT₂₀ and (h) PBAT tensile specimens.

specimens. However, it is worth noting that the glass transitions of PBAT disappeared nearly completely on $\tan \delta$ curves of PLA_xPBAT_y specimens, as their PBAT contents are equal to 2.5 wt % [Fig. 3(b)]. Only at PBAT contents equal to or higher than 5 wt %, distinguished glass transitions of PBAT were observed on the $\tan \delta$ curves of PLA_xPBAT_y specimens, and their magnitudes increase significantly

with the increase in PBAT contents [Fig. 3(c–g)]. On the other hand, it is interesting to note that the dynamic T_g values of PLA molecules reduce significantly from 73.8 to 69.5°C, as the PBAT contents of PLA_xPBAT_y specimens increase from 0 to 2.5 wt %. However, they increase reversely from 69.5 to 71.9 and 72.7°C, as the PBAT contents of PLA of PLA_xPBAT_y specimens increase from 2.5 to 5 and 20 wt %, respectively.

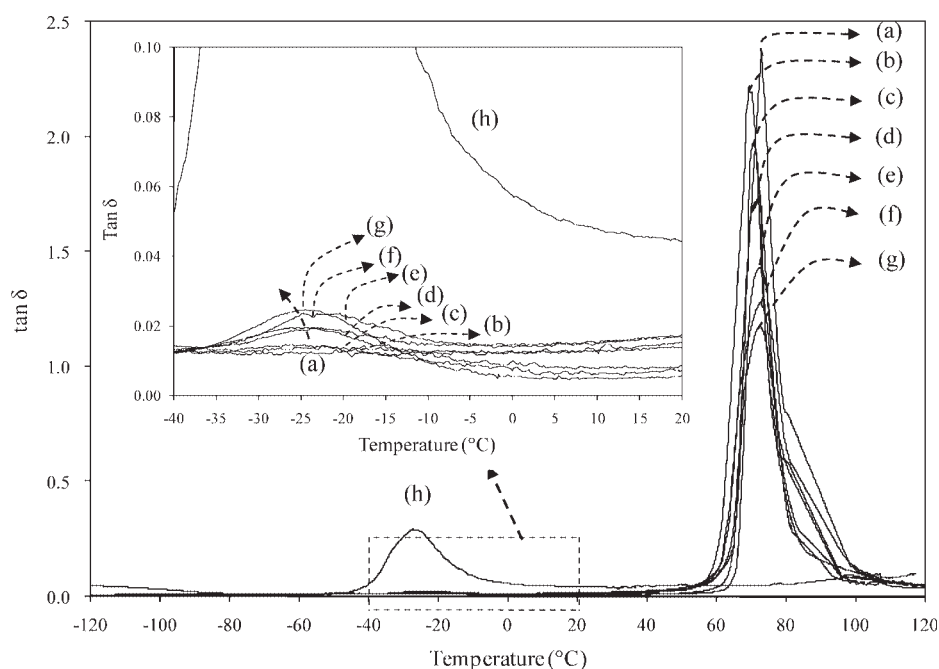


Figure 3 $\tan \delta$ curves of (a) PLA, (b) PLA_{97.5}PBAT_{2.5}, (c) PLA₉₅PBAT₅, (d) PLA_{92.5}PBAT_{7.5}, (e) PLA₉₀PBAT₁₀, (f) PLA₈₅PBAT₁₅, (g) PLA₈₀PBAT₂₀, and (h) PBAT specimens scanned at 3°C/min.

respectively. In contrast, the dynamic T_g values of PBAT of $\text{PLA}_x\text{PBAT}_y$ specimens reduce from -22.4 to -25.1°C , as their PBAT contents increase from 5 to 20 wt %.

Similar to the statement made in the previous section, these DMA results support the idea that PBAT and PLA molecules are miscible in the molecular level as the PBAT contents present in $\text{PLA}_x\text{PBAT}_y$ specimens are equal to or less than 2.5 wt %. Presumably, the significant reduction in dynamic glass transition temperatures of PLA with increasing PBAT contents is attributed to the compatible behavior between PLA and PBAT molecules, since PBAT molecules with much lower dynamic T_g values can somewhat reduce the dynamic T_g values of PLA-rich phases before phase separation at PBAT contents equal to or more than 5 wt %. On the contrary, the increase and reduction in dynamic T_g values of PLA and PBAT with further increasing PBAT contents is ascribed to the occurrence of phase-separated behavior between PLA and PBAT molecules at PBAT contents higher than 5 wt %, wherein the excess amounts of PBAT molecules not only invert but also bring additional PBAT molecules originally present in the PLA-rich phases into phase-separated PBAT particles. As a consequence, the dynamic T_g values of PLA and PBAT increase and reduce significantly, respectively, as the PBAT contents of $\text{PLA}_x\text{PBAT}_y$ specimens increase from 5 to 20 wt %.

The storage moduli (E') of PLA, $\text{PLA}_x\text{PBAT}_y$ and PBAT specimens were summarized in Figure 4. As shown in Figure 4(a,h), the E' values of PLA and PBAT specimens reduce significantly as their temperatures increase from 60 to 80°C and -40 to -20°C , respectively. The T_g values of glass transitions accompanied by a sharp reduction in E' of $\text{PLA}_x\text{PBAT}_y$ specimens reduce as their PBAT contents increase. Similar to those found in our previous investigation,³⁶ a significant rise on storage modulus (E') was found on the rubbery plateau of the PLA specimens. The E' values of PLA specimen increase by almost 10-folds as the temperatures increase from 98 to 117°C . Similar increase in E' values on the rubbery plateau of $\text{PLA}_x\text{PBAT}_y$ specimens was observed after blending varying amounts of PBAT in PLA, however, the onset temperatures corresponding to the increase in E' values shift to lower temperatures as the PBAT contents of $\text{PLA}_x\text{PBAT}_y$ specimens increase from 0 to 20 wt %. Moreover, the magnitudes of E' values arose on the rubbery plateau of $\text{PLA}_x\text{PBAT}_y$ specimens reduce significantly as their PBAT contents increase [Fig. 4(b–g)]. For instance, the E' values of $\text{PLA}_{80}\text{PBAT}_{20}$ specimen increase by only 1.4 times as the temperatures increase from 92 to 100°C . As evidenced in DSC analysis section, the X_c , T_m , and T_{onset} values of $\text{PLA}_x\text{PBAT}_y$ specimens reduce significantly as their PBAT contents increase.

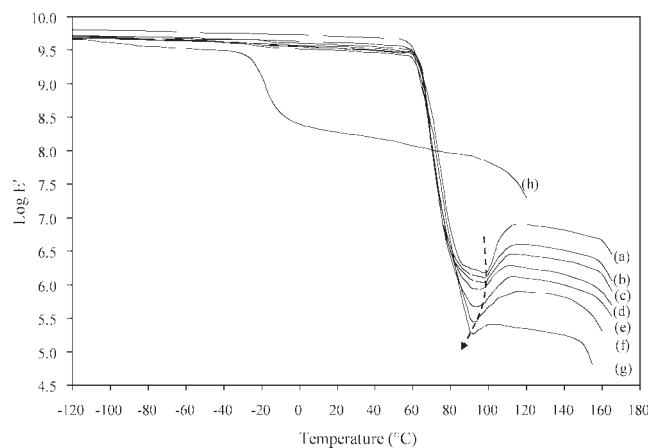


Figure 4 Storage modulus (E') curves of (a) PLA, (b) $\text{PLA}_{97.5}\text{PBAT}_{2.5}$, (c) $\text{PLA}_{95}\text{PBAT}_5$, (d) $\text{PLA}_{92.5}\text{PBAT}_{7.5}$, (e) $\text{PLA}_{90}\text{PBAT}_{10}$, (f) $\text{PLA}_{85}\text{PBAT}_{15}$, (g) $\text{PLA}_{80}\text{PBAT}_{20}$, and (h) PBAT specimens scanned at $3^\circ\text{C}/\text{min}$.

Based on these premises, it is reasonable to infer that the significant increase in E' values of PLA and $\text{PLA}_x\text{PBAT}_y$ specimens in their rubbery plateau regions is attributed to the re-crystallization of PLA crystals during their heat-scanning processes.

Wide angle X-ray diffraction properties

Typical wide angle X-ray diffraction patterns (WAXD) and peak diffraction angles of hot-pressed PLA and $\text{PLA}_x\text{PBAT}_y$ specimens are shown in Figure 5. A small diffraction peak centered at $2\theta = 17^\circ$ were found on the diffuse amorphous hump of the WAXD patterns of the PLA specimen [Fig. 5(a)]. These diffraction peaks are very similar to the diffraction patterns of α form PLA crystals reported in the literatures,^{37–41} and hence, are ascribed to the α form PLA crystals formed during the melt crystallization processes of the PLA specimen. Similar to those found in the literature,^{42,43} insignificant diffraction peaks centered at $2\theta = 16.4^\circ$, 17.8° , 21.7° , 23.3° , and 25.3° were found on the WAXD patterns of the PBAT specimen [Fig. 5(h)]. Presumably, these small diffraction peaks are originated from the formation of small amounts of poor PBAT crystals during the melt crystallization processes of the PBAT specimen. After blending PBAT in PLA resins, the small diffraction peaks originally corresponding to α form PLA and PBAT crystals centered at $2\theta = 17^\circ$ and 21.7° , respectively, were found on the WAXD patterns of all $\text{PLA}_x\text{PBAT}_y$ specimens. However, it is worth noting that the magnitude of diffraction peak centered at $2\theta = 17^\circ$ corresponding to α form PLA crystals reduces gradually as the PBAT contents of $\text{PLA}_x\text{PBAT}_y$ specimens increase. In contrast, another insignificant diffraction peak centered at 23.1° corresponding to PBAT crystals was found on the WAXD

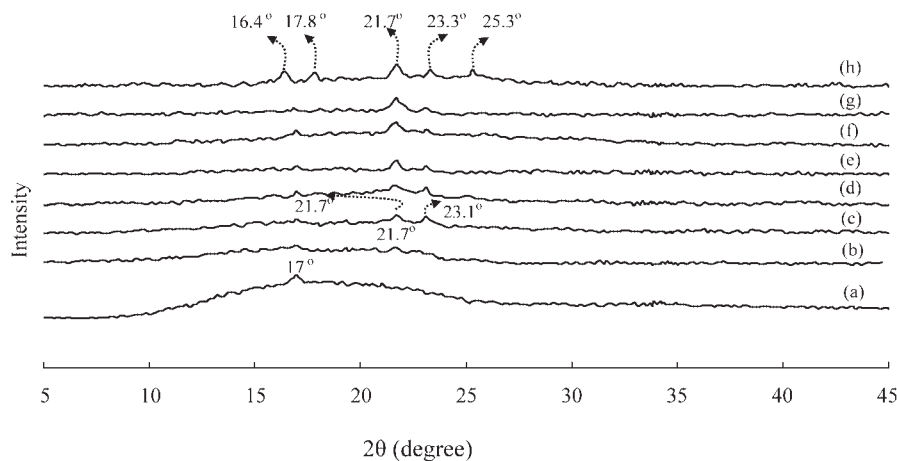


Figure 5 Wide angle X-ray diffraction patterns of hot-pressed (a) PLA, (b) PLA_{97.5}PBAT_{2.5}, (c) PLA₉₅PBAT₅, (d) PLA_{92.5}PBAT_{7.5}, (e) PLA₉₀PBAT₁₀, (f) PLA₈₅PBAT₁₅, (g) PLA₈₀PBAT₂₀, and (h) PBAT specimen.

patterns of PLA_xPBAT_y specimens, as their PBAT contents are equal to or more than 5 wt % [Fig. 5(c–g)]. In consistent with those found in DSC thermal analysis, the insignificant diffraction peaks found on the WAXD patterns of PLA, PBAT, and PLA_xPBAT_y specimens reveal that only small amounts of poor PLA and/or PBAT crystals are present in these melt crystallized specimens. Moreover, the gradually diminished diffraction peaks of α form PLA crystals of PLA_xPBAT_y specimens with increasing PBAT contents further support the idea that the melted PBAT molecules can inhibit the nucleation and crystallization of PLA molecules during their melt-crystallization processes.

Tensile properties analysis

The tensile properties of PLA_xPBAT_y specimens are summarized in Figure 6. The PLA specimen exhibits relatively high tensile strength (σ_f) at 58.6 MPa but

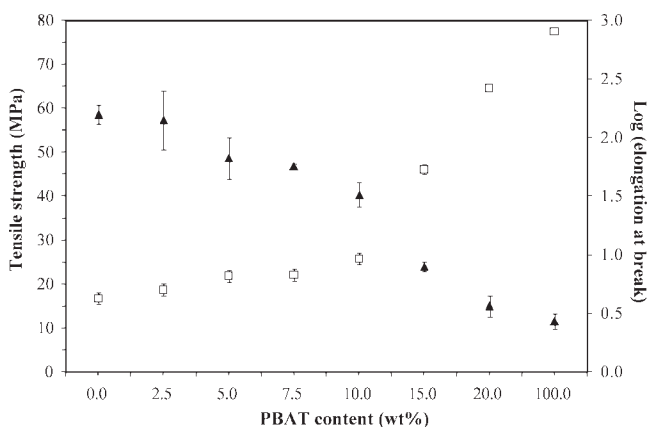


Figure 6 Tensile properties of PLA_xPBAT_y specimens with varying PBAT contents.

low elongation at break (ϵ_f) of 4.3%. In contrast, the PBAT specimen exhibits relatively low tensile strength (σ_f) at 11.6 MPa but particular high elongation at break (ϵ_f) of 811%. After blending PBAT in PLA, the PLA_xPBAT_y specimens revealed substantial reduction in σ_f values but increase in ϵ_f values as their PBAT contents increase. For example, the σ_f and ϵ_f values of PLA_xPBAT_y specimens reduce and increase from 58.6 to 40.2 and 23.0 MPa and from 4.3 to 9.5 and 266.0%, respectively, as their PBAT contents increase from 0 to 10 and 20 wt %, respectively. These results clearly suggest that the inherent brittle deformation behavior of the PLA specimen was successfully improved after blending proper amounts of PBAT in PLA resins.

CONCLUSIONS

Distinct glass temperature transition, melting endotherms and re-crystallization exotherms were found on the DSC and DMA thermograms of the PLA specimen. After blending PBAT in PLA, the X_c , T_m , and T_{onset} values of PLA_xPBAT_y specimens reduce gradually as their PBAT contents increase. In consistent with those found in DSC thermal analysis, the insignificant diffraction peaks found on the WAXD patterns of PLA, PBAT and PLA_xPBAT_y specimens reveal that only small amounts of poor PLA and/or PBAT crystals are present in their corresponding melt crystallized specimens. Nevertheless, the magnitudes of the diffraction peaks of α form PLA crystals of PLA_xPBAT_y specimens reduce gradually with increasing PBAT contents. On the other hand, the magnitudes corresponding to the re-crystallization and increase in E' values of PLA_xPBAT_y specimens reduce consistently as their PBAT contents increase. Further morphological and DMA analysis reveal that PBAT molecules are miscible

with PLA molecules at PBAT contents equal to or less than 2.5 wt %, since no distinguished phase-separated PBAT droplets and $\tan \delta$ transitions were found on the fracture surfaces and $\tan \delta$ curves of $\text{PLA}_x\text{PBAT}_y$ specimens, respectively. However, at PBAT contents higher than 2.5 wt %, distinguished phase-separated droplets and $\tan \delta$ of PBAT molecules become more clearly on the corresponding fracture surfaces and $\tan \delta$ curves of $\text{PLA}_x\text{PBAT}_y$ specimens, as their PBAT contents increase. In contrast, it is worth noting that the T_g values of PLA molecules found by DSC and DMA analysis reduce to the minimum value as the PBAT contents of $\text{PLA}_x\text{PBAT}_y$ specimens reach 2.5 wt %. The reversely increase in T_g values of PLA and PBAT with further increasing PBAT contents is ascribed to the occurrence of phase-separated behavior between PLA and PBAT molecules at PBAT contents higher than 2.5 wt %, wherein the excess amounts of PBAT molecules not only invert but also bring additional PBAT molecules originally present in the PLA-rich phases into phase-separated PBAT particles. In contrast to PLA, the PBAT specimen exhibits relatively low σ_f but particular high ϵ_f value. After blending proper amounts of PBAT in PLA, the inherent brittle deformation behavior of the PLA specimen was successfully improved.

References

- Joo, Y. N.; Masami, O.; Hirotaka, O.; Mitsuru, N.; Arimitsu, U.; Masatoshi, M. *Polymer* 2006, 47, 1340.
- Li, H.; Michel, A. H. *Polymer* 2007, 10, 1016.
- Kulinski, Z.; Piorkowska, E. *Polymer* 2005, 46, 10290.
- Hu, Y.; Hu, Y. S.; Topolkarayev, V.; Hiltner, A.; Baer, E. *Polymer* 2003, 44, 5681.
- Lai, W. C.; Liao, W. B.; Lin, T. T. *Polymer* 2004, 45, 3073.
- Piorkowska, E.; Kulinski, Z.; Galeski, A.; Masirek, R. *Polymer* 2006, 47, 7178.
- Pluta, M.; Galeski, A. *J Appl Polym Sci* 2002, 86, 1386.
- Rashkov, I.; Manolova, N.; Li, S. M.; Espartero, J. L.; Vert, M. *Macromolecules* 1996, 29, 50.
- Chen, X. H.; McCarthy, S. P.; Gross, R. A. *Macromolecules* 1997, 30, 4295.
- Maglio, G.; Migliozi, A.; Palumbo, R. *Polymer* 2003, 44, 369.
- Chon, D.; Hotovely-Salomon, A. *Polymer* 2005, 46, 2068.
- Nijenhuis, A. J.; Colstee, E.; Grijpma, D. W.; Pennings, A. J. *Polymer* 1996, 37, 5849.
- Choi, N. S.; Kim, C. H.; Cho, K. Y.; Park, J. K. *J Appl Polym Sci* 2002, 86, 1892.
- Na, Y. H.; He, Y.; Shuai, X.; Kikkawa, Y.; Doi, Y.; Inoue, Y. *Biomacromolecules* 2002, 3, 1179.
- Wang, L.; Ma, W.; Gross, R. A.; McCarthy, S. P. *Polym Degrad Stab* 1998, 59, 161.
- Dell'Erba, R.; Groeninckx, G.; Maglio, G.; Malinconico, M.; Migliozi, A. *Polymer* 2001, 42, 7831.
- Chen, C. C.; Chueh, J. Y.; Tseng, H.; Huang, H. M.; Lee, S. Y. *Biomaterials* 2003, 24, 2297.
- Yang, J. M.; Davé, V.; Gross, R. A.; McCarthy, S. P. *Polym* 1996, 37, 437.
- Park, J. W.; Im, S. S. *Polymer* 2003, 44, 4341.
- Blümm, E.; Owen, A. J. *Polymer* 1995, 36, 4077.
- Zhang, L. L.; Deng, X. M.; Zhao, S. J.; Huang, Z. T. *J Appl Polym Sci* 1997, 65, 1849.
- Focarete, M. L.; Scandola, M.; Dobrzynski, P.; Kowalczyk, M. *Macromolecules* 2002, 35, 8472.
- Zhang, L. L.; Xiong, C. D.; Deng, X. M. *Polymer* 1996, 37, 235.
- Koyama, N.; Doi, Y. *Polymer* 1997, 38, 1589.
- Ohkoshi, I.; Abe, H.; Doi, Y. *Polymer* 2000, 41, 5985.
- Park, J. W.; Im, S. S. *J Polym Sci Part B: Polym Phys* 2002, 40, 1931.
- Park, J. W.; Im, S. S. *J Appl Polym Sci* 2002, 86, 647.
- Xu, Y.; Hanna, M. A. *Carbohydr Polym* 2005, 59, 521.
- Witt, U.; Einig, T.; Yamamoto, M.; Kleeberg, I.; Deckwer, W. D. *Chemosphere* 2001, 44, 298.
- Yoshihiro, S.; Yuichi, S.; Mitsuhiro, S. *J Appl Polym Sci* 2005, 95, 386.
- Jiang, L.; Wolcott, M. P.; Zhang, J. *Biomacromolecules* 2006, 7, 199.
- Liu, T. Y.; Lin, W. C.; Yang, M. C.; Chen, S. Y. *Polymer* 2005, 46, 12586.
- Fischer, E. W.; Sterzel, H. J.; Wegner, G.; *Kolloid, Z. Z. Polymer* 1973, 251, 980.
- Rezgui, F.; Swistek, M.; Hiver, J. M.; G'Sell, C.; Sadoun, T. *Polymer* 2005, 46, 7370.
- Martin, O.; Avérous, L. *Polymer* 2001, 42, 6209.
- Yeh, J. T.; Huang, C. Y.; Chai, W. L.; Chen, K. N. *J Appl Polym Sci* 2009, 112, 2757.
- DeSantis, P.; Kovacs, A. J. *Biopolymers* 1968, 6, 299.
- Saha, S. K.; Tsuji, H. *Polym Degrad Stab* 2006, 91, 1665.
- Grijpma, D. W.; Zondervan, G. J.; Pennings, A. J. *Polym Bull* 1991, 25, 327.
- Zhong, W.; Ge, J.; Gu, Z.; Li, W.; Chen, X.; Zang, Y.; Yang, Y. *J Appl Polym Sci* 1999, 74, 2546.
- Solarski, S.; Ferreira, M.; Devaux, E. *Polymer* 2005, 46, 11187.
- Kuwabara, K.; Gan, Z.; Nakamura, T.; Abe, H.; Doi, Y. *Biomacromolecules* 2002, 3, 390.
- Kang, H. J.; Park, S. S. *J Appl Polym Sci* 1999, 72, 593.